SAND2022-7159C

Sandia National Laboratories

Thermal Performance of Multistage Falling Particle Receiver at Various Commercial Scales

Jae Bok (Samuel) Lee and Brantley Mills

ASME 16th International Conference on Energy Sustainability

July 11th – 13th 2022

U.S. DEPARTMENT OF ENERGY | NNSA

Sandia National Laboratories is a multimission laboratory managed and operated by National Technology & Engineering Solutions of Sandia, LLC, a wholly owned subsidiary of Honeywell International Inc., for the U.S. Department of Energy's National Nuclear Security Administration under contract DE-NA0003525.

Sandia National Laboratories is a multimission laboratory managed and operated by National Technology & Engineering Solutions of Sandia, LLC, a wholly owned subsidiary of Honeywell International Inc., for the U.S. Department of Energy's National Nuclear Security Administration under contract DE-NA0003525.

Introduction

Free-falling particle receivers (FFPRs)

- Heat transfer fluids: Ceramic particles (i.e. CARBO HSP, sand, etc).
- Advantages: Direct irradiance, high particle temperature (>1000°C), cost-effectiveness
- Disadvantages: High advective losses, short particle residence time, dispersive particle curtain

NSTTF FFPR test loop in 2018

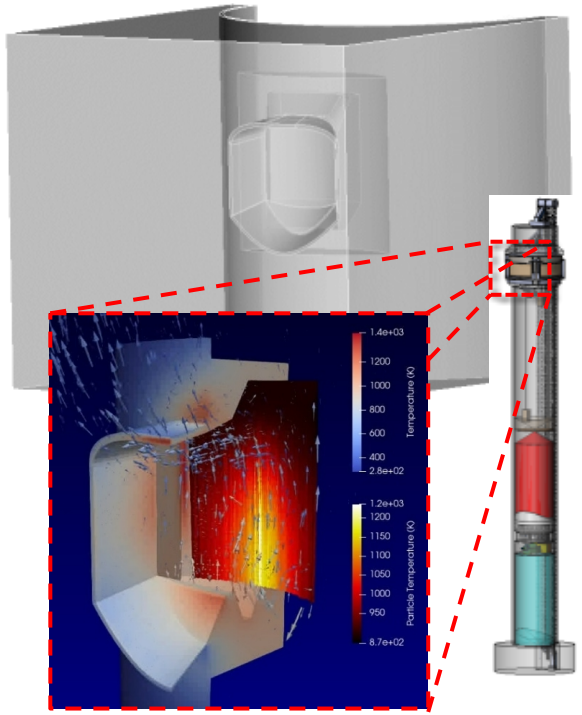

Candidate commercial scale FFPR design

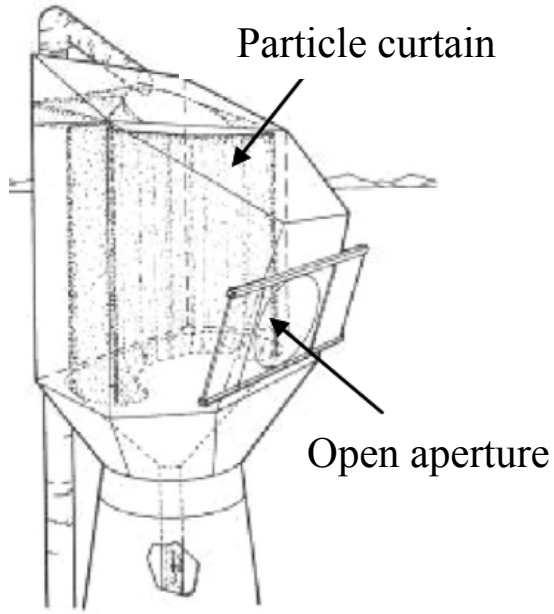

Ho (2014)

Multistage Receivers

Multistage falling particle receiver (MFPR)

- Stable particle curtain, longer particle residence time, lower advective losses

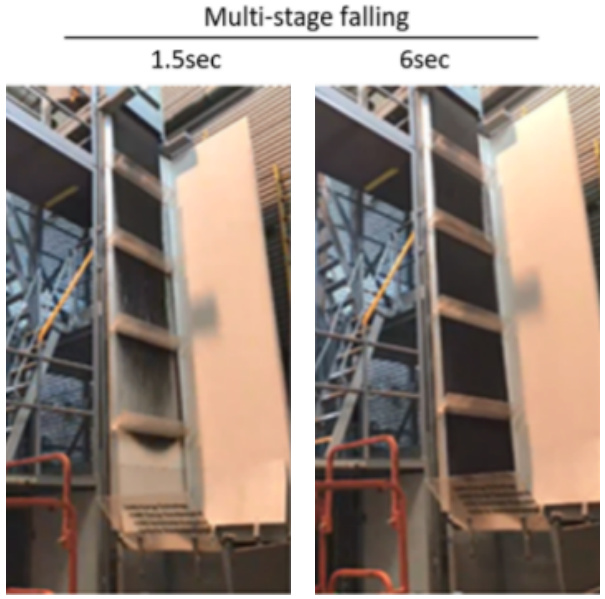

Kim *et al.* (2019)

Yue *et al.* (2020)

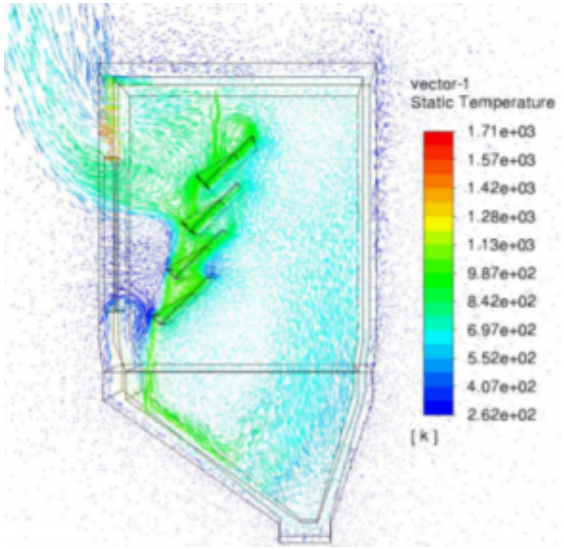

Shaeffer *et al.* (2020)

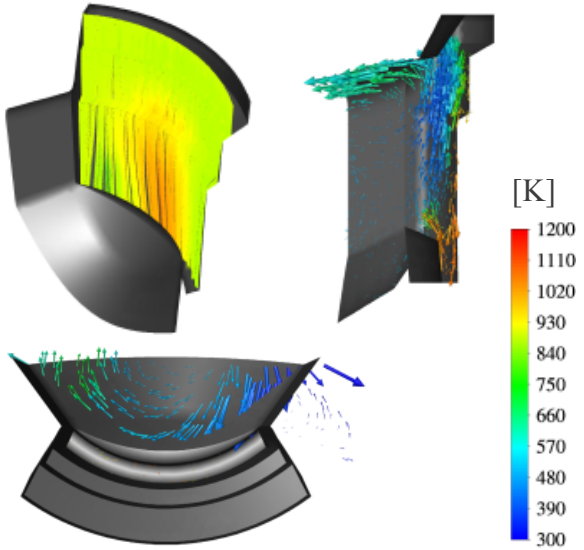

Lee and Mills (2021)

Still requires

(1) High-performing MFPR design in terms of thermal efficiency

(2) Investigation of MFPR performance at various commercial scales

(3) Investigation of MFPR performance under realistic environment (i.e. cloud cover, wind)

Objectives

1. To develop a high performing commercial scale MFPR geometry
2. To investigate the MFPR performance at various commercial scales
3. To investigate the MFPR performance at various incident solar heat fluxes and wind conditions
4. To develop a robust correlation to predict the thermal performance of a MFPR

1. Higher thermal performance compared to a similar free-falling particle receiver (FFPR)
2. Better predictions of the MFPR performance at various commercial scales
3. Better predictions of the MFPR efficiency in realistic environmental conditions (e.g. cloud cover)
4. Correlation can be integrated into technoeconomic analyses

Computational model

Cubit

- Geometry/mesh generation

ANSYS Fluent®

- Material properties of CARBO HSP particles (~350 μm)
- Eulerian-Lagrangian model for the particle-laden flow
- Realizable k-ε turbulence model
- Fluid-thermal coupling
- Non-grey discrete ordinate radiation model for radiative heat transfer
- Forward velocity (~0.3m/s) for trough angle of 30° [Shaeffer *et al.* (2020)]
- Particle drag model: Morsi & Alexander (1972)

Simulation parameters

- Wind directions: N ~ SW
- Wind speeds (U_w): 0 ~ 15m/s
- Aperture area (A_p): 25, 144, 324m^2
- Incident solar radiative flux (Q_{in}/A_p): 0 ~ 3MW/m^2
- Inlet temperature: 888.15K
- Particle mass flow rate: 178kg/s (A_p=25m^2), 885.5kg/s (A_p=144m^2), 2864kg/s (A_p=324m^2)

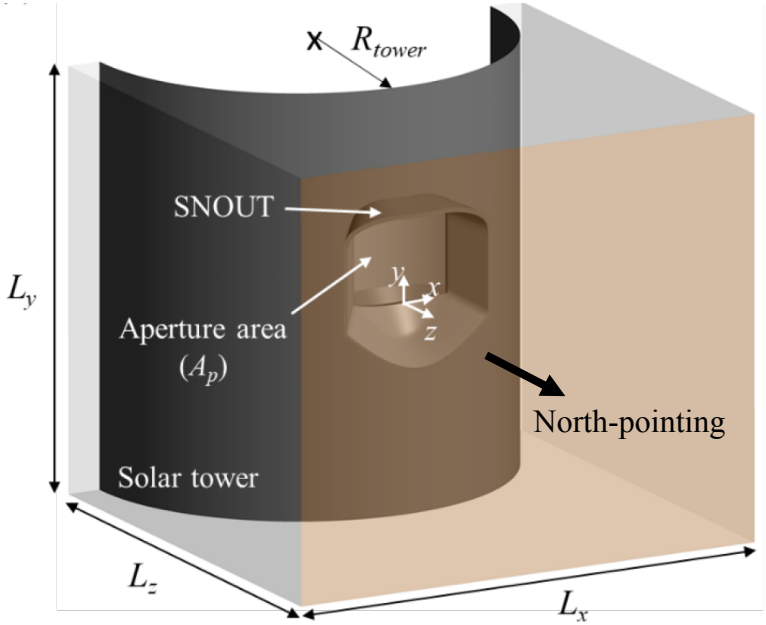

Computational domain

Wind directions

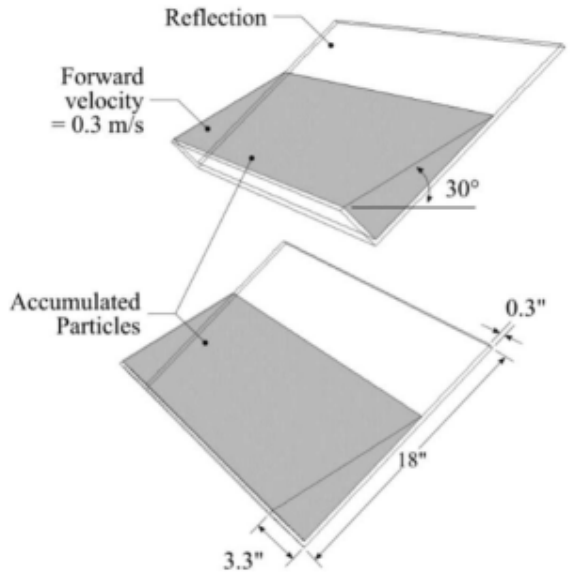

Shaeffer *et al.* (2020)

Improved thermal performance with a MFPR

- Starting with a proposed high-performing 100MW$_e$ FFPR geometry
- Incident solar power (Q_{in}) of 200MW; Aperture area (A_p) of 144m^2; Particle mass flow rate: 885.5kg/s
- Best performing MFPR geometry: s_1=12m, s_2=8m, l_1=2m, l_2=1m [Lee and Mills (2021]
- Maximum MFPR efficiency: **~88% (5%-points greater than the FFPR efficiency)**

Schematic diagram of FFPR

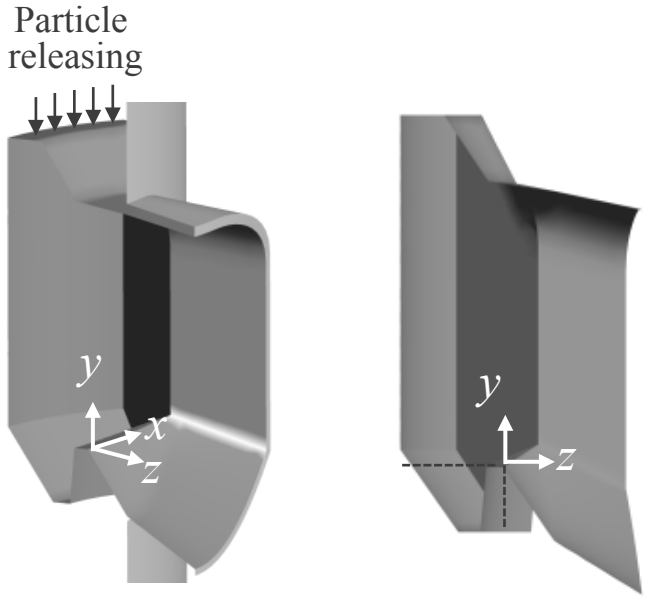

Schematic diagram of MFPR

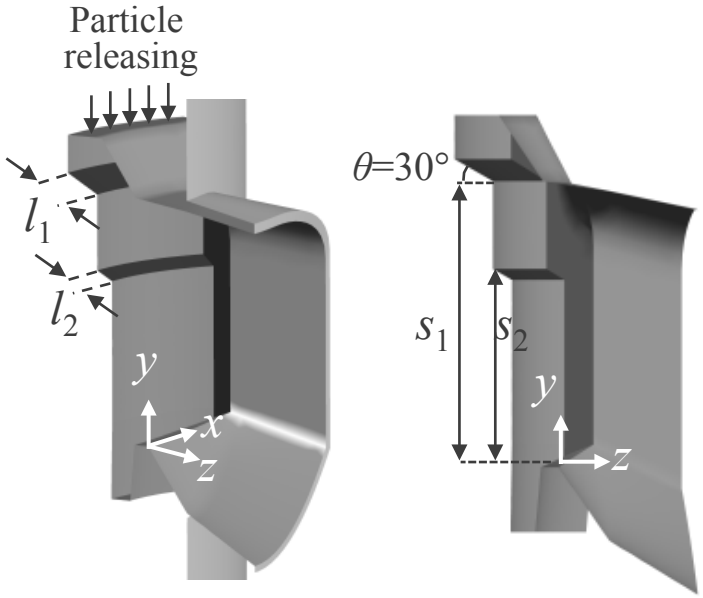

Comparison of flow and temperature fields between FFPR and MFPR

FFPR

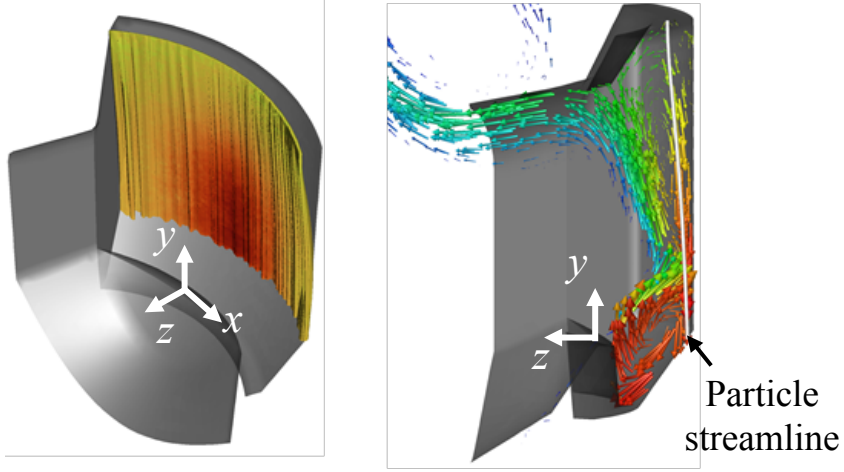

MFPR

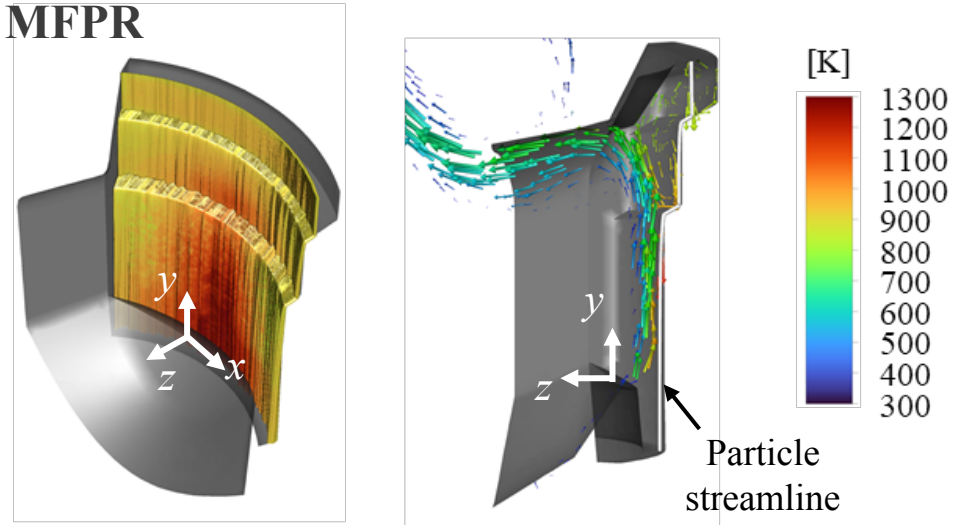

Velocity (z) profiles

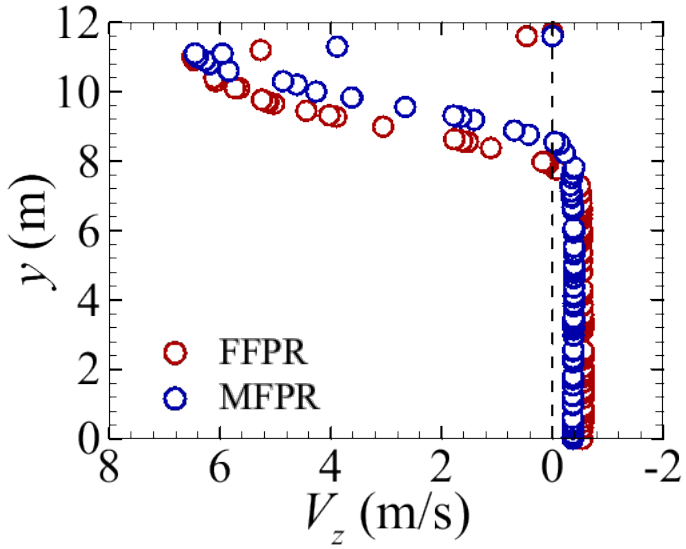

Temperature profiles

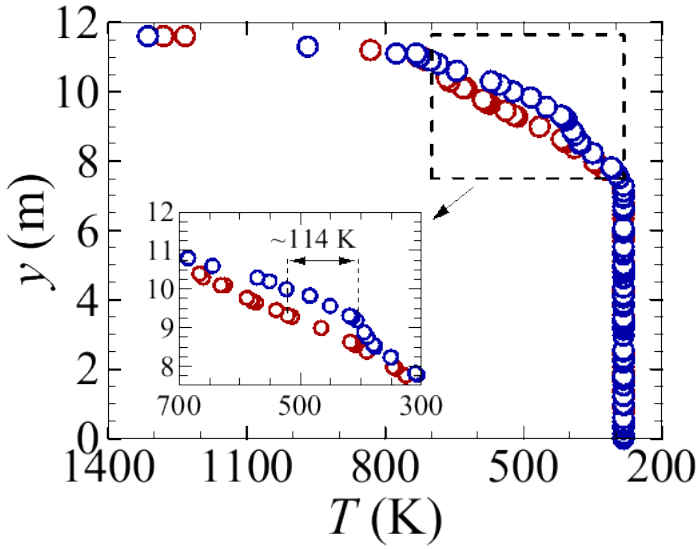

MFPR performance for various incident solar heat flux (Q_{in}/A_p)

Increasing incident solar heat flux ($Q_{in}/A_p \uparrow$)

- Increasing magnitude of Q_{abs}
- Marginal variations in Q_{adv} and Q_{rad}
- Lower proportion of the thermal losses ($Q_{loss}/Q_{in} \downarrow$)

Marginal change

$\frac{Q_{loss}}{Q_{in}}$

Increasing

Q_{abs} vs Q_{in}/A_p

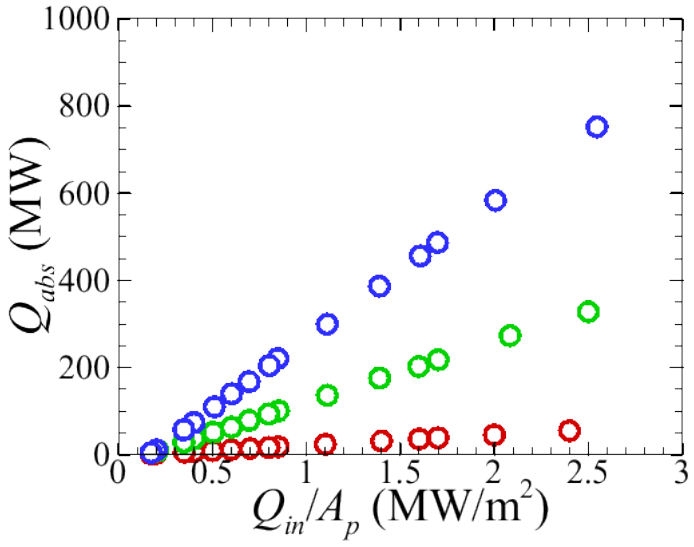

Q_{adv} vs Q_{in}/A_p

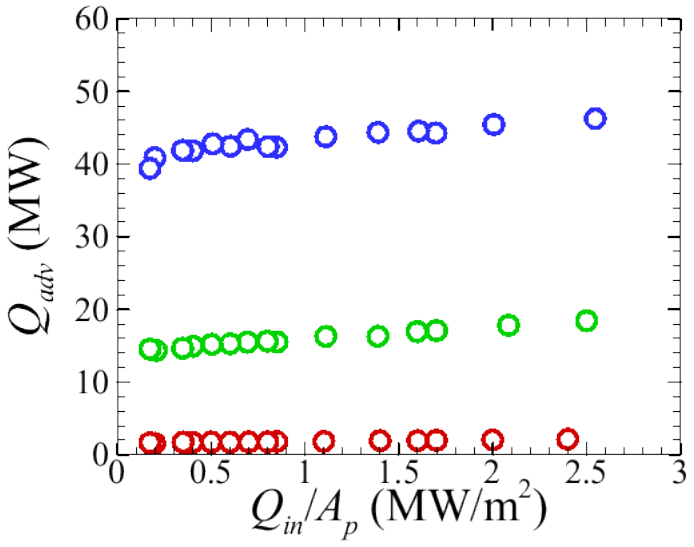

Q_{rad} vs Q_{in}/A_p

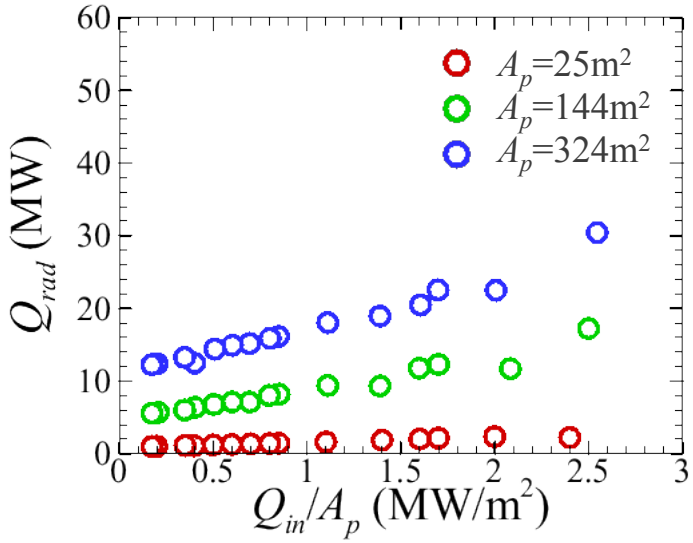

MFPR performance for various incident solar heat flux (Q_{in}/A_p)

Increasing incident solar heat flux (Q_{in}/A_p↑)

- Increasing magnitude of Q_{abs}
- Marginal variations in Q_{adv} and Q_{rad}
- Lower proportion of the thermal losses (Q_{loss}/Q_{in}↓)

Marginal change

$\frac{Q_{loss}}{Q_{in}}$

Increasing

η (=Q_{abs}/Q_{in})vs Q_{in}/A_p

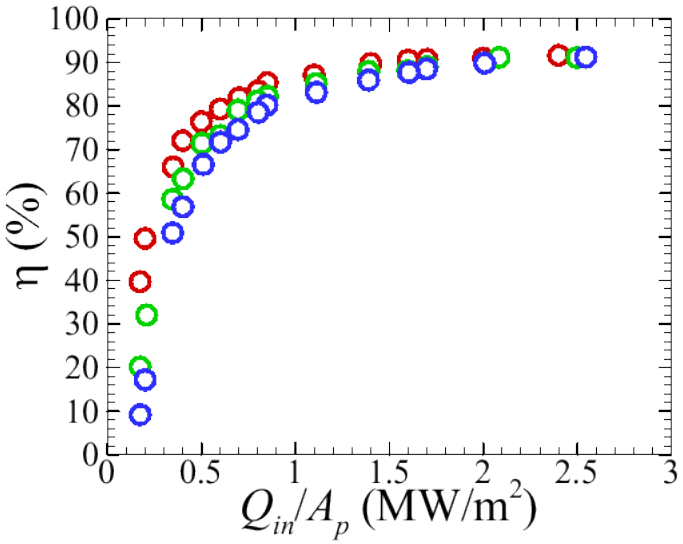

Q_{adv}/Q_{in} vs Q_{in}/A_p

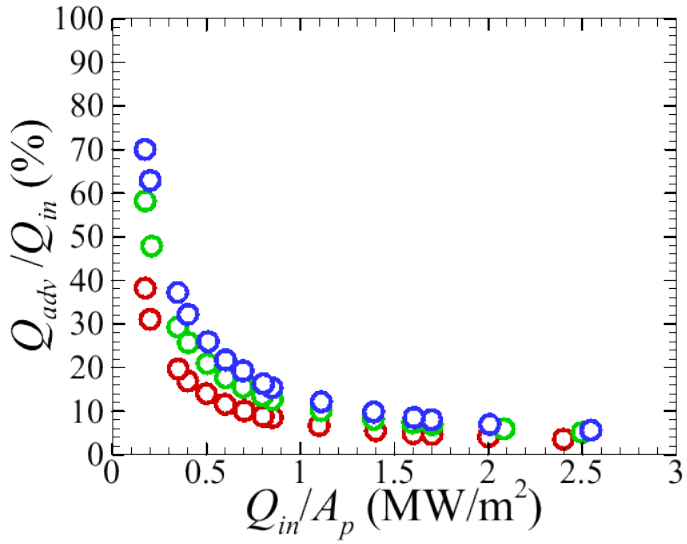

Q_{rad}/Q_{in} vs Q_{in}/A_p

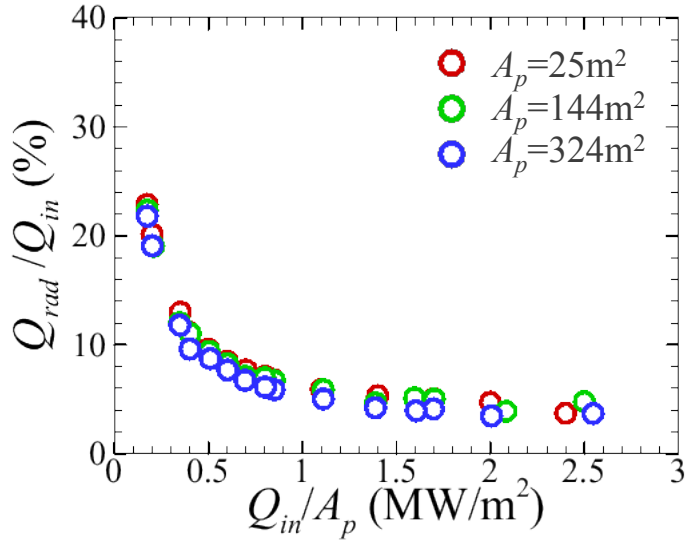

MFPR performance for various incident solar heat flux (Q_{in}/A_p)

Incident solar power scaled by A_p^m

- Data points of η and Q_{adv}/Q_{in} collapse with m =1.2
- Data points of η converge to ~90% at $Q_{in}/A_p^{1.2} \sim 0.75$ regardless of receiver scales

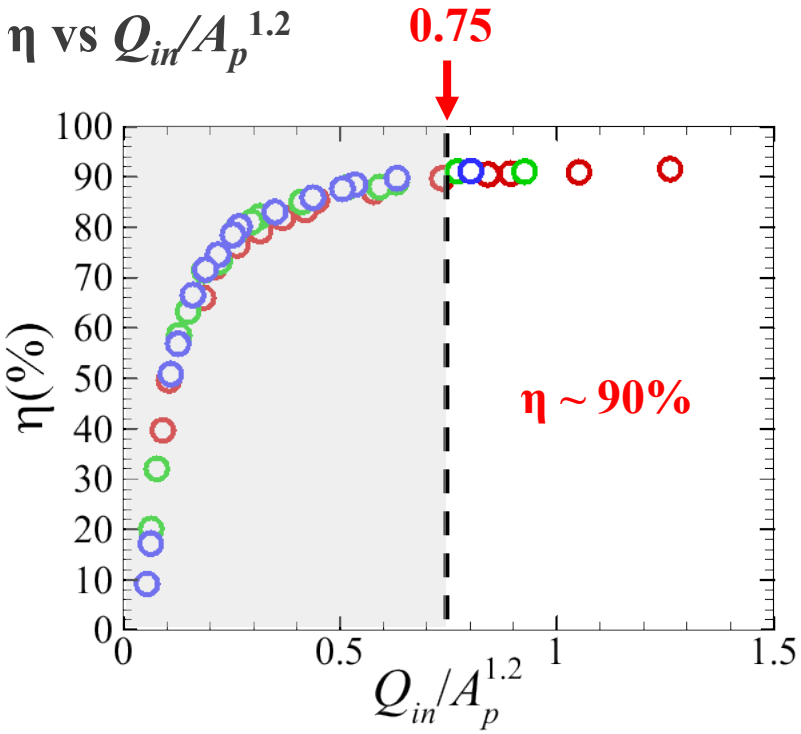

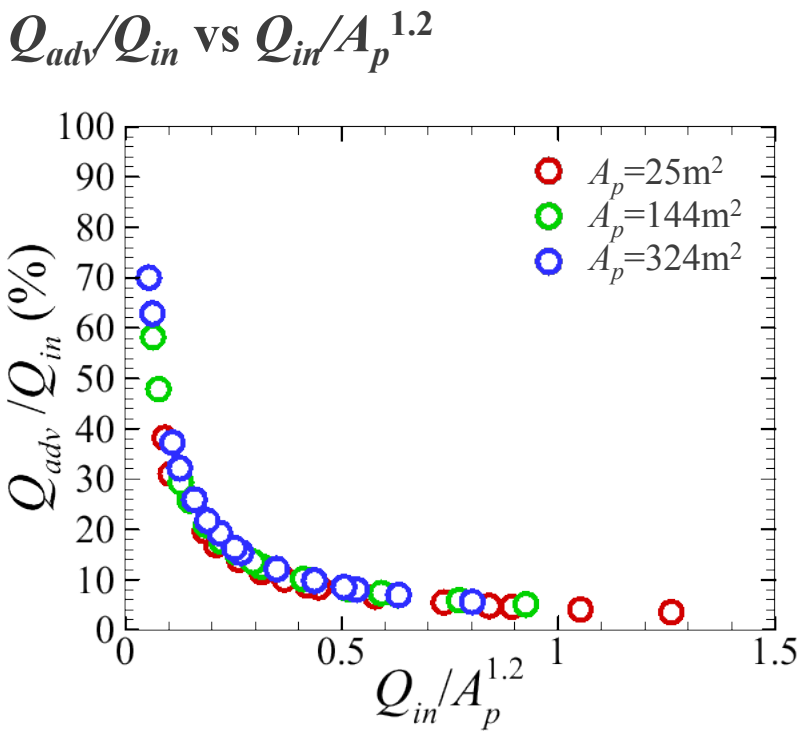

MFPR performance subject to wind

- Advective losses are the main source of efficiency degradation.
- NW or WNW winds are detrimental for thermal efficiency.
- Vortices existing ahead of open aperture intensify the advective loss.
- Effects of wind speed are significant for either NW or WNW winds.

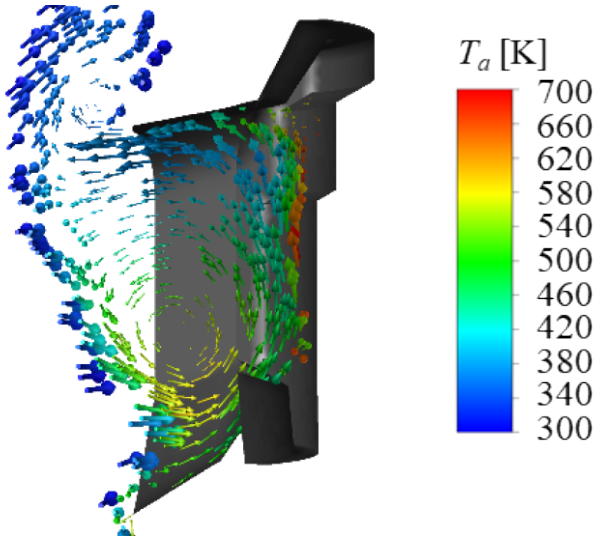

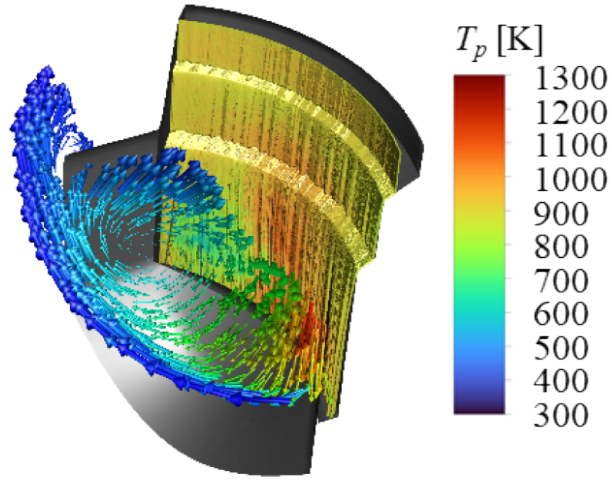

NW wind (315°) ,
V_w=15m/s, Q_{in}=100MW$_{th}$

η vs wind direction

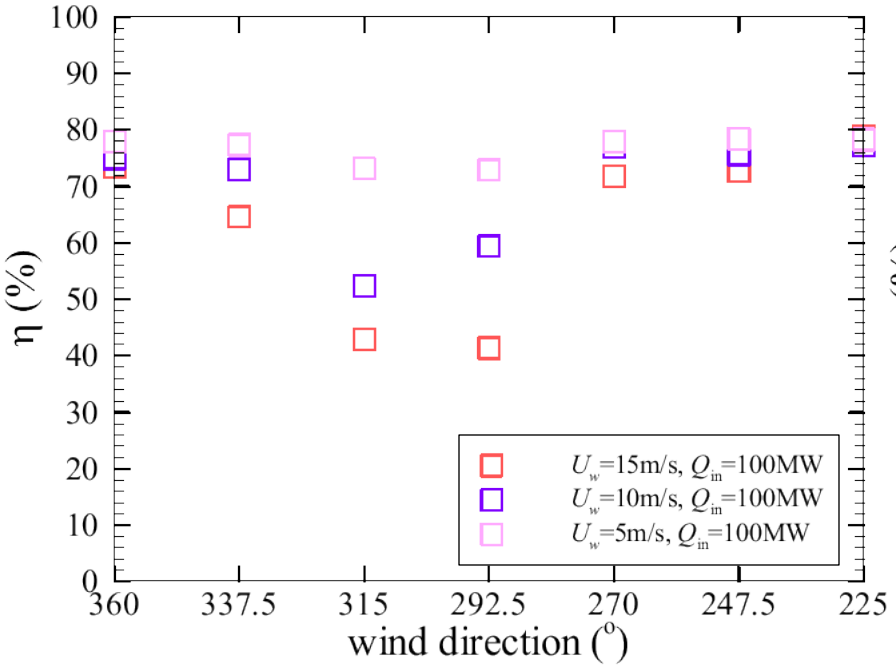

Q_{adv}/Q_{in}, Q_{rad}/Q_{in} vs wind direction

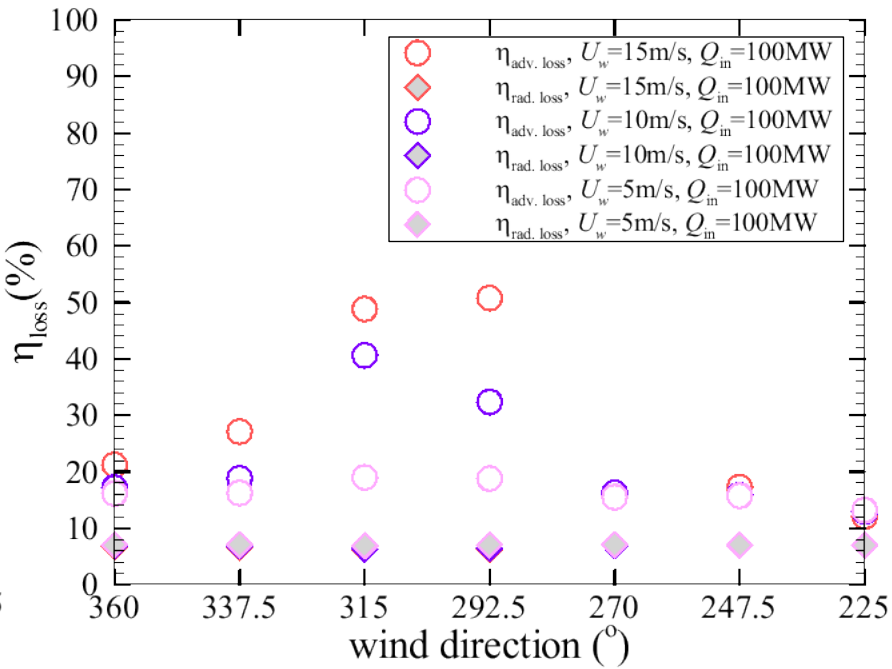

MFPR efficiency subject to wind at various scales

Parametric study

- NW or WNW winds are detrimental for thermal efficiency.
- Effects of wind speed are significant for either NW or WNW winds.

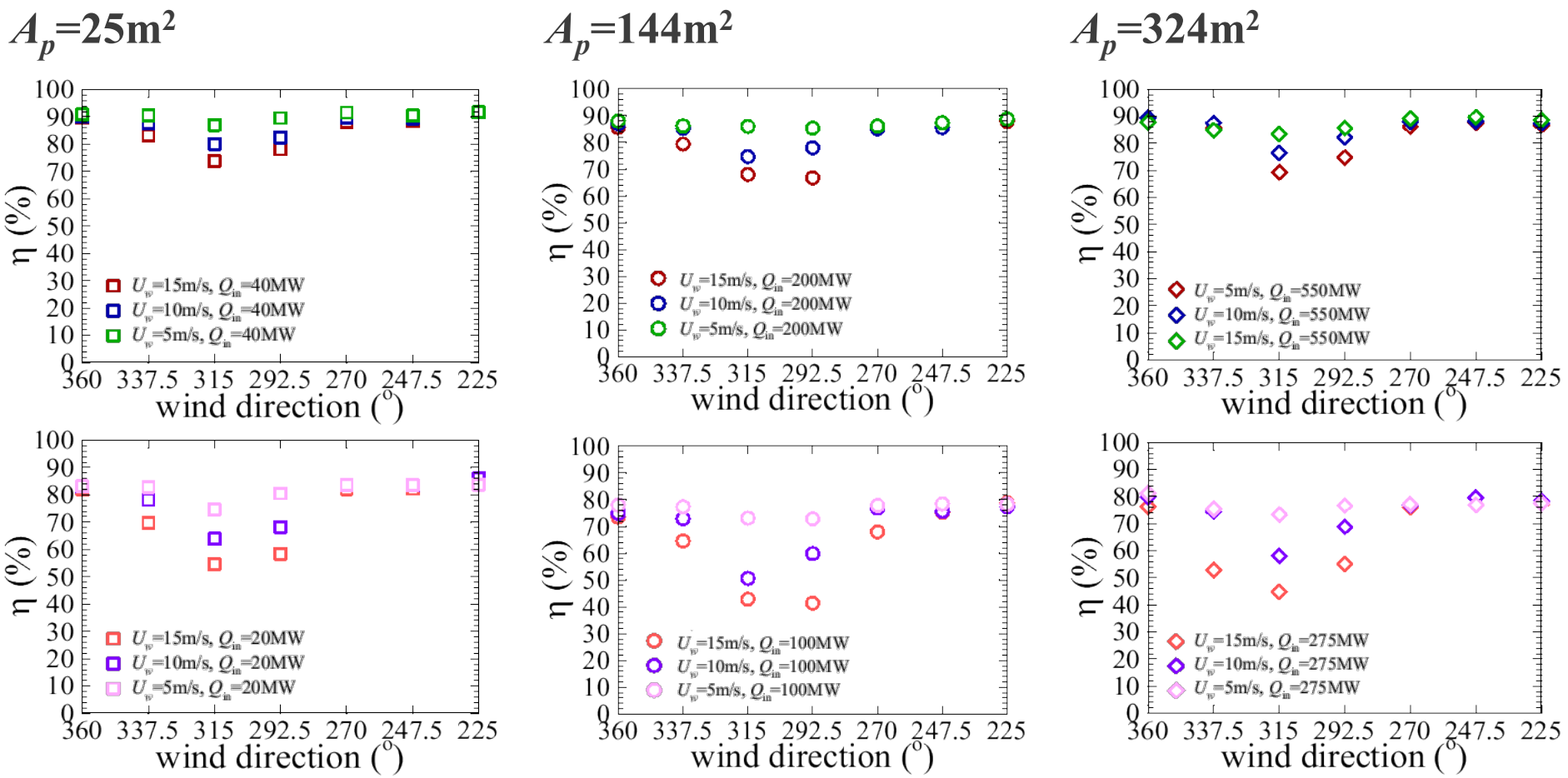

Correlation development

- Incident solar power (Q_{in}), wind speeds (U_w), wind directions (θ_w), Aperture area (A_p)
- Correlation function: $A + B\tilde{q} + C\tilde{q}^2 + D\tilde{q}U_w\Theta + EU_w{}^2\Theta$

$$\text{where } \Theta = \frac{(180-|\theta_w-180|)^F}{H}\exp\left[-\left(\frac{180-|\theta_w-180|}{G}\right)\right] \text{ (Wind direction modifier)}$$

$$\tilde{q} = e^{-Q_{in}/A_p}$$

Correlation coefficients

	Efficiency	Advective Losses
A	0.9351	0.0021
B	-0.0560	0.1166
C	-0.5519	0.2940
D	-6.4055×10^{-5}	7.1750×10^{-5}
E	-3.1344×10^{-6}	2.7996×10^{-6}
F	5.0	5.0
G	9.1	9.1
H	5000	5000

Thermal efficiency (η)

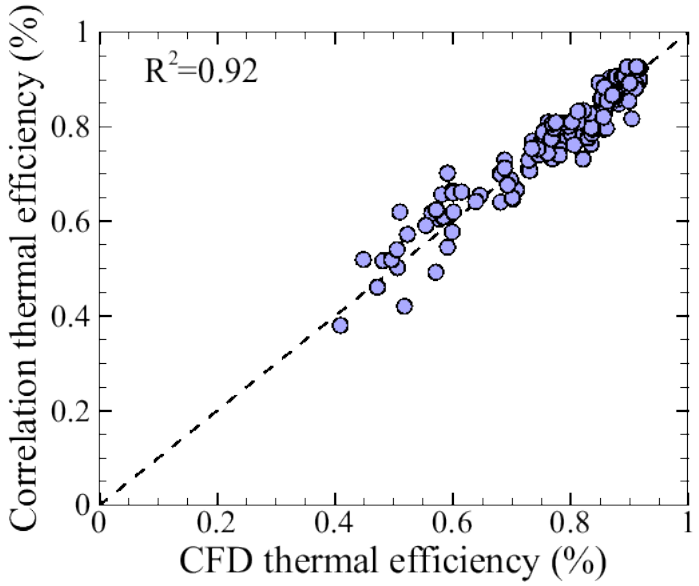

Advective loss (Q_{adv}/Q_{in})

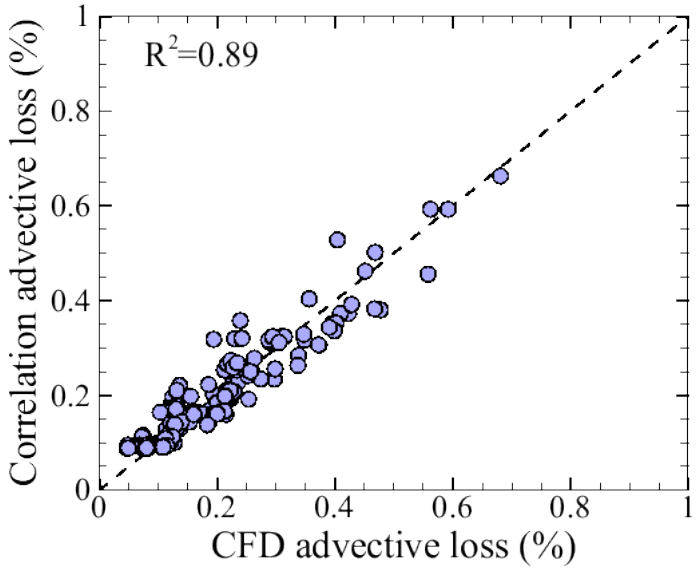

Summary and conclusions

❑ MFPR geometry in a quiescent condition

- The present MFPR geometry provides ~5% higher thermal efficiency compared to the given FFPR geometry.
- Thermal efficiency reaches ~90% at $Q_{in}/A_p^{1.2}$=0.75 regardless of receiver scales.

❑ MFPR efficiency under various wind conditions

- NW or WNW winds are detrimental for thermal efficiency.
- Entrainment of cooler ambient air into the receiver cavity becomes significant due to vortices existing ahead of the open aperture.
- Increasing wind speed intensifies the advective loss.

❑ Correlation development

- R-square value ~ 92%, which is sufficient to predict the thermal efficiency.
- Different parameter inputs also need to be investigated for robustness. (i.e. Particle inlet temperature)

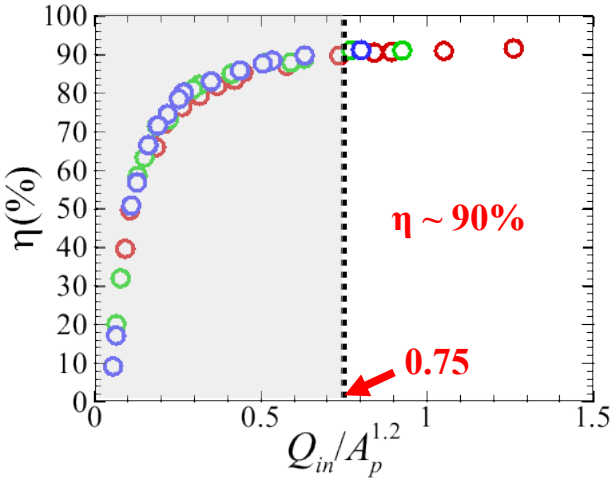

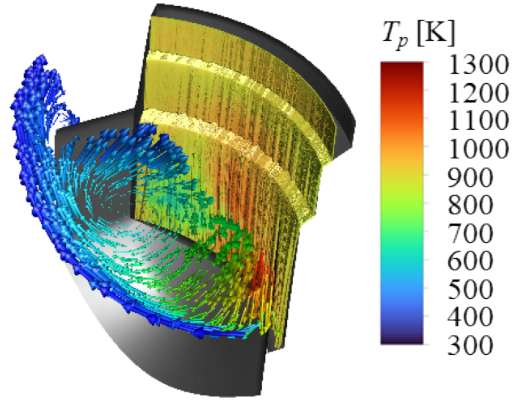

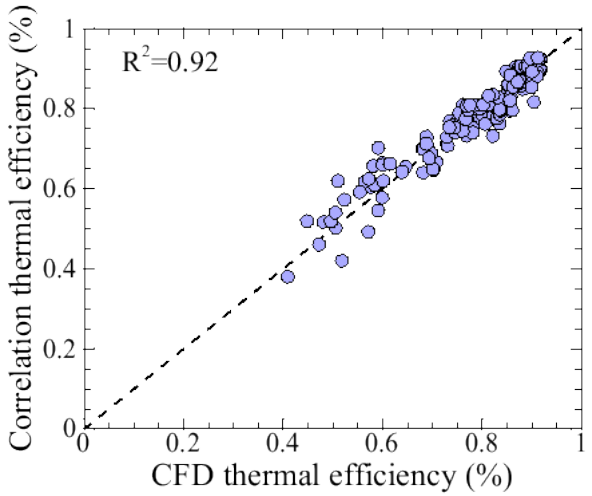

Acknowledgements

Sandia National Laboratories is a multi-mission laboratory managed and operated by National Technology and Engineering Solutions of Sandia, LLC., a wholly owned subsidiary of Honeywell International, Inc., for the U.S. Department of Energy's National Nuclear Security Administration under contract DE-NA0003525.

Thank you

Appendix

Improved thermal performance with a MFPR

- Starting with Sandia's candidate 100MW$_e$ FFPR geometry
- Incident solar power (Q_{in}) of 200MW; Aperture area (A_p) of 144m^2; Particle mass flow rate: 885.5kg/s
- Best performing MFPR geometry: s_1=12m, s_2=8m, l_1=2m, l_2=1m [Lee and Mills (2021]
- Maximum MFPR efficiency: ~88% (5% greater than FFPR efficiency at the same operating condition)

Schematic diagram of MFPR

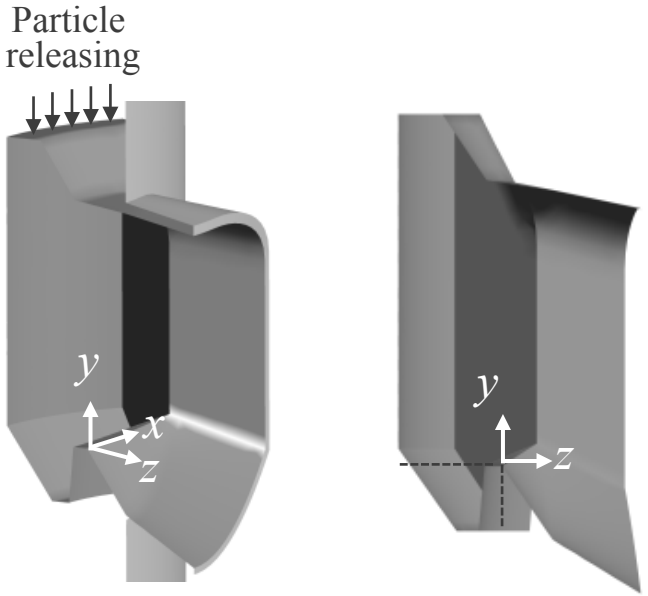

Schematic diagram of MFPR

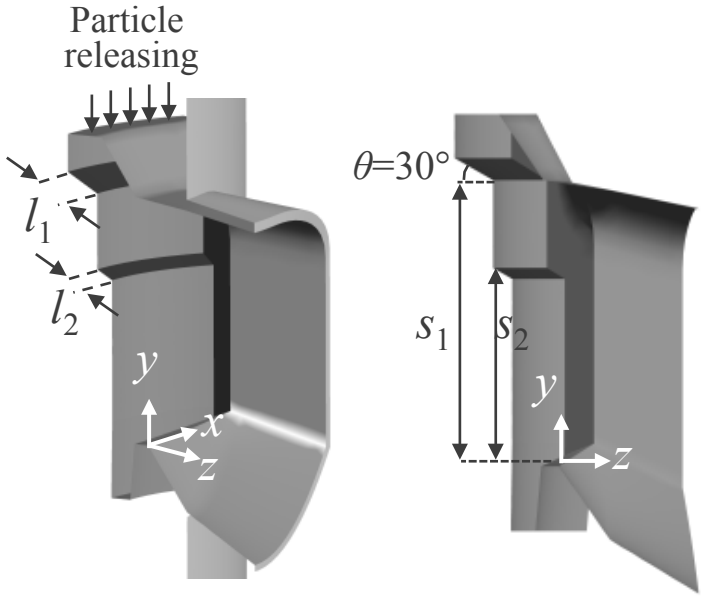

Incident solar radiative flux

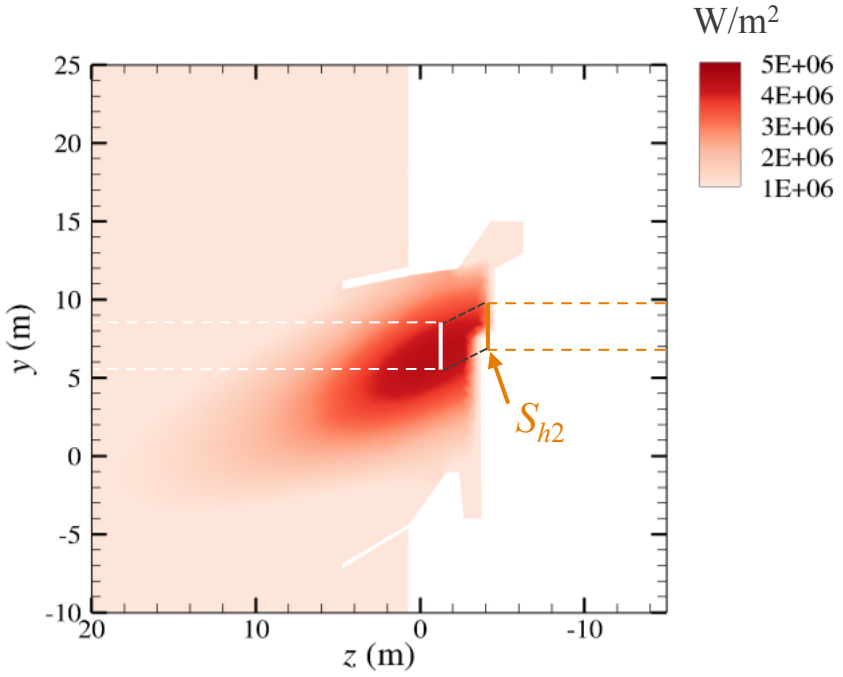

Improved thermal performance with a MFPR

- Thermal efficiency: Remarkably distinguished from whether the intermediate trough is positioned in S_{h2}
- Best performing MFPR geometry: s_1, s_2, l_1, l_2
- Maximum MFPR efficiency: ~88% (5% greater than FFPR efficiency)

Intermediate troughs should be placed around S_{h2}

Particle position (y_p)

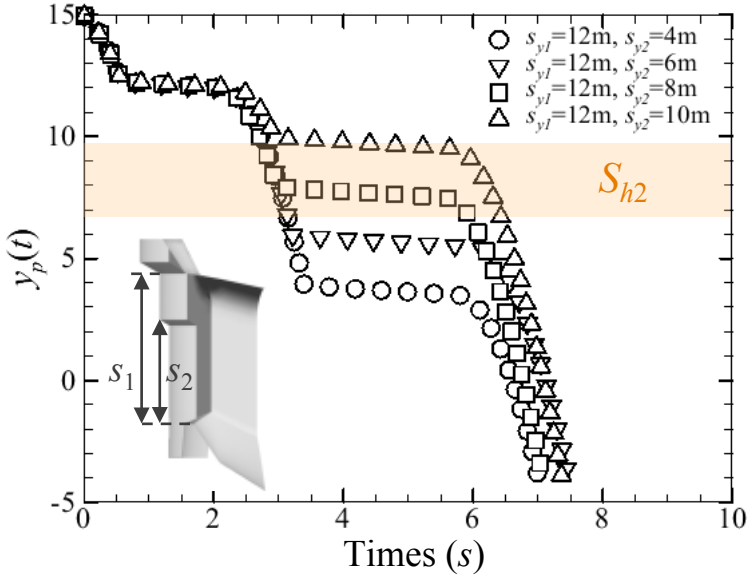

Thermal efficiency ($\eta = Q_{abs}/Q_{in}$)

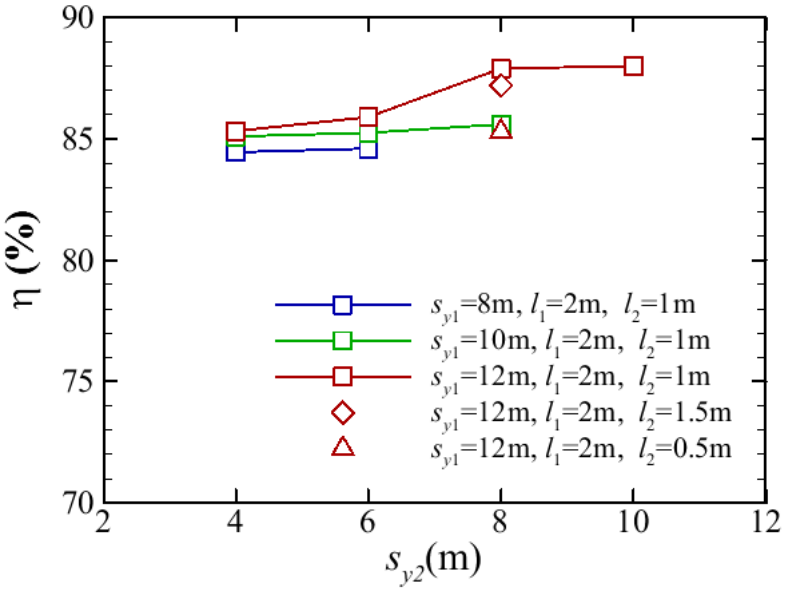

Thermal losses ($\eta_{loss} = Q_{loss}/Q_{in}$)